Contribution from 3M Corporate Research Laboratories, St. Paul, Minnesota 55144, and Department of Chemistry, University of Minnesota, Minneapolis, Minnesota 55455

Protonation of Transition-Metal Acetate and Hydrido Acetate Complexes with Fluorocarbon Acids

A. R. Siedle,*† R. A. Newmark,† G. A. Korba,† L. H. Pignolet,‡ and Paul D. Boyle‡

Received October 23, 1987

The reactions of a series of transition-metal hydrido acetate complexes with the fluorocarbon acid $H_2C(SO_2CF_3)_2$ have been studied. $(Ph_3P)_2Ru(CO)H(OAc)$ and $(Ph_3P)_2Ru(CO)Cl(OAc)$ yield cationic, binuclear $[(Ph_3P)_4Ru_2(CO)_2(\mu\text{-}X)(\mu\text{-}OAc)][HC(SO_2CF_3)_2]$ (X = H, Cl). Reaction of $(Ph_3P)_3RuH(OAc)$ with $H_2C(SO_2CF_3)_2$ in toluene forms $[(\pi\text{-toluene})RuH(PPh_3)_2][HC(SO_2CF_3)_2]$. The osmium complex $(Ph_3P)_3OsH(OAc)$ provides instead $[(Ph_3P)_3Os(\eta^2\text{-}H_2)(\eta^2\text{-}OAc)][HC(SO_2CF_3)_2]$·toluene in which a molecular hydrogen ligand has been characterized by its ^1H spin–lattice relaxation time and J_{HD} in the HD analogue. The crystal structure was determined but the $\eta^2\text{-}H_2$ ligand was not clearly resolved. Crystal data (at −63 °C): $P\bar{1}$ (triclinic), a = 14.780 (4) Å, b = 15.376 (5) Å, c = 13.854 (4) Å, α = 100.62 (2)°, β = 97.63 (2)°, γ = 77.36°, Z = 2, ρ = 1.557 g cm^{-3}, R = 0.036. Elimination of acetic acid and formation of *mer-trans*-$[(Ph_3P)_3OsH(CH_3CN)_2][HC(SO_2CF_3)_2]$ occurs on reaction with acetonitrile.

Introduction

We have previously described the reactions of fluorocarbon acids of the general type $RCH(SO_2R_f)_2$ (R_f = perfluoroalkyl) with a wide variety of transition-metal hydrides.[1-7] These acids exhibit an unusual collection of properties in that they are strong, nonoxidizing, nonhygroscopic carbon-centered acids that are soluble in apolar, nondonor solvents such as toluene and dichloromethane. Their conjugate bases are generally noncoordinating, and the carbon-bonded C–$HC(SO_2CF_3)_2$ ligand has been observed in only three cases, all involving Pt(II).[2] Use of these compounds makes possible the study of proton-transfer chemistry with minimal complications from coordination by solvent, conjugate bases, or adventitious water. This paper describes the protonation chemistry of a series of metal acetate and hydrido acetate complexes. We were curious to see whether, following protonation of an idealized hydrido acetate complex to form $MH_2(OAc)^+$, hydrogen or acetic acid would be eliminated (eq 1).

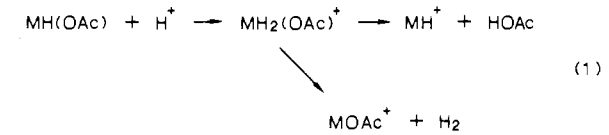

(1)

Results

Reaction of $(Ph_3P)_2Ru(CO)_2(OAc)_2$ with 1 equiv of $H_2C(SO_2CF_3)_2$ in toluene at 80 °C yields $[(Ph_3P)_2Ru(CO)_2(OAc)][HC(SO_2CF_3)_2]\cdot C_7H_8$, (**1**). The ^{31}P NMR spectrum comprises a singlet at 33.3 ppm, and the infrared spectrum in CH_2Cl_2 displays two carbonyl stretching bands at 2020 and 2065 cm^{-1}. These data suggest that **1** contains, as is usually the case for this $4d^6$ element, octahedrally coordinated Ru(II) with trans Ph_3P ligands, cis carbonyl groups, and a bidentate acetate moiety. In this and other compounds reported here, it is, in principle, possible to ascertain the mode of acetate coordination from analysis of those C–O stretching frequencies that do not overlap other bands in the infrared spectrum. However, this strategy has recently been challenged,[8] and since we have no new data that can resolve the issue, we prefer to use NMR data and reasonable assumptions about metal coordination number preference to assess acetate coordination. The presence of ionic $HC(SO_2CF_3)_2^-$ in **1** is revealed by the characteristic 3.86 ppm singlet in the ^1H NMR spectrum and by the conductance in CH_2Cl_2, 35 Ω^{-1} cm^2 mol^{-1}.[5] Formation of **1** may be viewed as involving protonation followed by reductive elimination of acetic acid. A similar sequence obtains for $(Ph_3P)_3Rh(OAc)$, which forms the 14-electron rhodium(I) compound $[(Ph_3P)_3Rh][HC(SO_2CF_3)_2]$ (**2**), but the reaction is of no preparative value for the starting acetate is prepared from acetic acid and $(Ph_3P)_4RhH$, which itself reacts with $H_2C(SO_2CF_3)_2$ to yield **2**.[1,3,7]

Reaction of $(Ph_3P)_2Ru(CO)H(OAc)$ with $H_2C(SO_2CF_3)_2$ yields brown, microcrystalline $[(Ph_3P)_4Ru_2(CO)_2(\mu\text{-}H)_2(\mu\text{-}OAc)][HC(SO_2CF_3)_2]$ (**3**), ν_{CO} = 1973 cm^{-1}. The binuclear nature of this compound is indicated by the ^1H NMR spectrum, which shows a poorly resolved triplet hydride resonance at −11.3 ppm. The ^{31}P NMR spectrum in acetone-d_6, which discloses an apparent 35-Hz doublet centered at 39.4 ppm (cf. Figure 1), is unusual in that it shows no absorption between the two very intense doublet components but does show two weak outside peaks. These spectra are attributable, on account of the magnetic nonequivalence of ^{31}P and ^1H nuclei, to an $A_2A'_2XX'$ spin system, where A and A′ refer to geminal ^{31}P nuclei on the same Ru center, a plausible representation if $^4J_{PP}$ is assumed to be zero. The spectra were analyzed utilizing a literature procedure for an AA′XX′ system[9] followed by calculations with the Varian XL spectral simulation computer package for an $A_2A'_2XX'$ system taking $J_{AA'}$ = 20 Hz, close to the typical 15 Hz value. To the resolution obtained, it was not necessary to invoke a more complex spin system in which there is significant P–Ru–H–Ru–P coupling. The calculated spectra match within experimental error the observed spectra, but the coupling constants must be regarded as approximate because of suboptimal resolution in the latter. The analysis yields J_{PH} = 46, $J_{P'H}$ = −9 (note that these two couplings are required to have opposite signs), $J_{PP'}$ = 20, and $J_{HH'}$ = 0 Hz. The analytical procedure does not distinguish between $J_{PP'}$ and $J_{HH'}$, but assignment of a near-zero value to the latter is justified because $J_{HH'}$ in crystallographically characterized $[(Ph_3P)_4Ru_2(CO)_2(\mu\text{-}H)_2(\mu\text{-}CF_3SO_2)][HC(SO_2CF_3)_2]$, which we consider to be structurally similar, yields a first-order ^1H NMR spectrum in which $J_{HH'}$ is unambiguously determined to be 2.5 Hz.[4]

An analogous binuclear Ru(II) complex, $[(Ph_3P)_4Ru_2(CO)_2(\mu\text{-}Cl)_2(\mu\text{-}OAc)][HC(SO_2CF_3)_2]$ (**4**), ν_{CO} = 1973 cm^{-1}, is formed from $(Ph_3P)_2Ru(CO)Cl(OAc)$ and $H_2C(SO_2CF_3)_2$. We consider that **3** is analogous to $[(Ph_3P)_4Ru_2(CO)_2(\mu\text{-}H)_2(\mu\text{-}CF_3SO_2)][HC(SO_2CF_3)_2]$[4] and to $[(Ph_3P)_4Ru_2(CO)_2(\mu\text{-}Cl)(\mu\text{-}H)_2][HC(SO_2CF_3)_2]$, the latter being obtained from $(Ph_3P)_2Ru(CO)HCl$

† 3M Corporate Research Laboratories.
‡ University of Minnesota.

(1) Siedle, A. R.; Newmark, R. A.; Pignolet, L. H.; Howells, R. D. *J. Am. Chem. Soc.* **1984**, *106*, 1510.
(2) Siedle, A. R.; Newmark, R. A.; Gleason, W. B. *J. Am. Chem. Soc.* **1986**, *108*, 767.
(3) Siedle, A. R.; Newmark, R. A.; Pignolet, L. H. *Organometallics* **1984**, *3*, 855.
(4) Siedle, A. R.; Newmark, R. A.; Pignolet, L. H. *Inorg. Chem.* **1986**, *25*, 1345.
(5) Siedle, A. R.; Newmark, R. A.; Pignolet, L. H., *Inorg. Chem.* **1986**, *25*, 3412. The value for T_1 of Os–*H* in $[(Ph_3P)_4OsH_3][HC(SO_2CF_3)_2]$ at −87 °C should read 670 ms.
(6) Siedle, A. R.; Newmark, R. A.; Pignolet, L. H.; Wang, D. X.; Albright, T. A. *Organometallics* **1986**, *5*, 38.
(7) Siedle, A. R.; Howells, R. D., U.S. Pat. 4556720.
(8) Deacon, G. B.; Huber, F.; Phillips, R. J. *Inorg. Chim. Acta* **1985**, *104*, 41.
(9) Emsley, J. W.; Feeney, J.; Sutcliffe, L. H. *High Resolution Nuclear Magnetic Resonance Spectroscopy*; Pergamon: London, 1965; p 392.

0020-1669/88/1327-1593$01.50/0

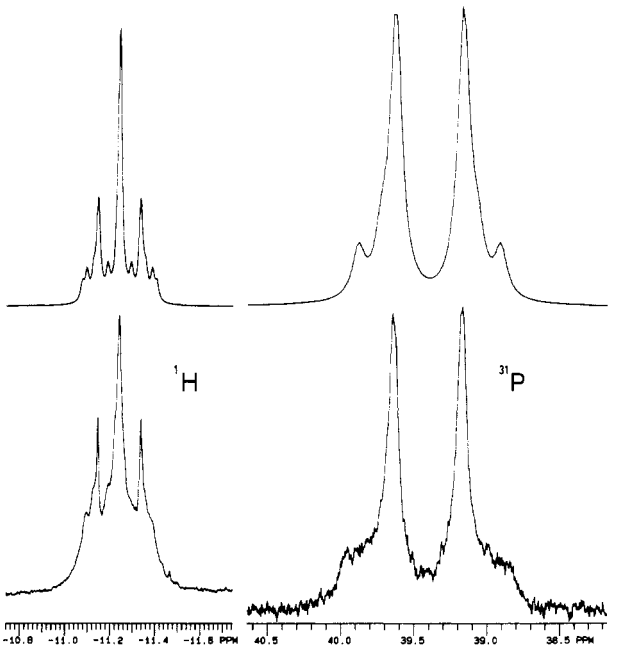

Figure 1. Calculated (upper) and observed (lower) ^{1}H and ^{31}P NMR spectra of $[(Ph_3P)_4Ru_2(CO)_2(\mu\text{-}H)_2(\mu\text{-}OAc)][HC(SO_2CF_3)_2]$.

and $H_2C(SO_2CF_3)_2$.[6] Then, **3** and **4** are simply related by replacement of the two bridging hydrides by chloride.

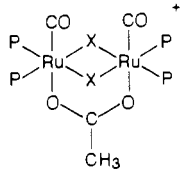

3, X = H
4, X = Cl

In toluene, $(Ph_3P)_3RuH(OAc)$ and $H_2C(SO_2CF_3)_2$ react to form $[(\eta^6\text{-tol})RuH(Ph_3P)_2][HC(SO_2CF_3)_2]$ (tol = toluene).[10] This compound is one of an extensive series of cationic ruthenium(II) arene complexes of the type $(arene)RuH(PPh_3)_2^+$, originally obtained from $(Ph_3P)_4RuH_2$ and $H_2C(SO_2CF_3)_2$ in arene solvents, which has been studied by crystallographic and molecular orbital calculational methods.[6] Synthesis of other $(arene)RuH(PPh_3)_2^+$ complexes is readily accomplished by using the neat arene as solvent. Because the hydrido acetate complex $(Ph_3P)_3RuH(OAc)$ is more readily available than $(Ph_3P)_4RuH_2$ and because it gives higher yields of π-arene derivatives, particularly with arenes bearing electron-withdrawing substituents, it is the preferred starting material for these complexes.

The osmium analogue, $(Ph_3P)_3OsH(OAc)$, is protonated by $H_2C(SO_2CF_3)_2$ to yield $[(Ph_3P)_3Os(\eta^2\text{-}H_2)(\eta^2\text{-}OAc)][HC(SO_2CF_3)_2]$·tol (**5**), which, in toluene, shows no tendency to eliminate acetic acid and form $(tol)OsH(PPh_3)_2^+$ although such elimination does occur in more basic solvents (vide infra). The narrow-band ^{1}H-decoupled ^{31}P NMR spectrum of **5** at 50 °C discloses a poorly resolved triplet at 3.9 ppm, indicating the presence of two hydride ligands; any odd number is excluded because the resulting material would be paramagnetic. In addition, the ^{1}H NMR spectrum displays at ambient temperature a binomial quartet of relative area 2 at −8.9 ppm with J_{PH} = 9.5 Hz, indicating that the molecule is stereochemically nonrigid.

It is well-known that the spin–lattice relaxation time T_1 goes through a minimum when the Brownian motion, characterized by a correlation time τ, is best matched by the Larmor frequency and, most cases, NMR spectra are obtained in the extreme-narrowing regime where $\omega\tau \ll 1$. Crabtree has shown that the extreme-narrowing model is inappropriate for ^{1}H high-field NMR spectra of metal hydride protons and has developed a relationship between the H–H distance in transition-metal polyhydrides and the minimum value of T_1 when it is plotted as a function of temperature.[11] T_1 for the Os–*H* protons in **5**, measured at 9.4 T on a degassed 3.7×10^{-2} M solution in CD_2Cl_2, varies from 57 ms at +22 °C to 76 ms at −87 °C with a minimum of 41 ms near −35 °C. These short values are within the range reported for η^2-H_2 complexes,[11] and d(H–H) is calculated to be 1.11 Å. For comparison, T_1 for the Os–*H* protons in the η^1-H compound $[(Ph_3P)_4OsH_3][HC(SO_2CF_3)_2]$ (3.5×10^{-2} M in CD_2Cl_2) is 355 ms at +22 °C and 670 ms at −87 °C, with T_1(min) being 295 ms at −24 °C, indicating that d(H–H) is 1.55 Å.[5]

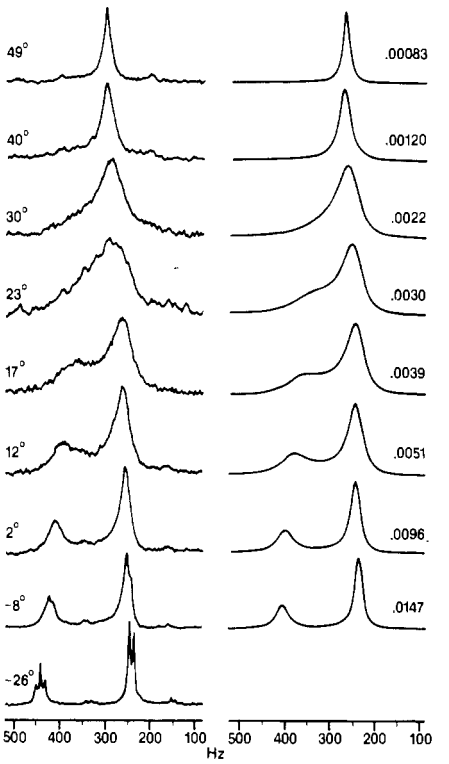

Figure 2. Observed (left, temperature in °C) and calculated (right, lifetimes in s) ^{31}P DNMR spectra of $[(Ph_3P)_3Os(\eta^2\text{-}H)_2(\eta^2\text{-}OAc)][HC(SO_2CF_3)_2]$.

The presence in **5** of coordinated molecular hydrogen is supported by the ^{2}H NMR spectrum of $[(Ph_3P)_3Os(\eta^2\text{-}HD)(\eta^2\text{-}OAc)][PhC(SO_2CF_3)_2]$, obtained from $(Ph_3P)_3OsH(OAc)$ and $PhCD(SO_2CF_3)_2$. In this, the −8.9 ppm resonance appears as a doublet corresponding to an H–D coupling of 13.7 Hz, which implies that H and D are covalently bonded. This value is smaller than that found in $(i\text{-}Pr_3P)_2W(HD)(CO)_3$, 33.5 Hz,[12] or $(Ph_3P)_2Ir(H)(H_2)$(7,8-benzoquinolinate)$^+$, 29.5 Hz,[11] but is still very much larger than obtains for $M(\eta^1\text{-}H)_2$ derivatives.

The $^{31}P\{^1H\}$ NMR spectrum of $[(Ph_3P)_3Os(\eta^2\text{-}H_2)(\eta^2\text{-}OAc)][HC(SO_2CF_3)_2]$ at −26 °C reveals a doublet at δ 2.9 and a triplet at δ 5.8 with $J_{PP'}$ = 10 Hz. These resonances coalesce with increasing temperature in a manner typical of a dynamic, intramolecular exchange process between two distinguishable sites of relative populations 2:1; cf. Figure 2. Spectra were calculated[13] for two sites of unequal populations undergoing rapid exchange. Free energies of activation, $\Delta G^{\ddagger}$, were calculated from absolute reaction rate theory. The linear dependence of $\Delta G^{\ddagger}$ on T (from 13.26 kcal/mol at −9 °C to 14.38 kcal/mol at +50 °C) yields $\Delta H^{\ddagger} = 8.3 \pm 0.6$ kcal/mol and $\Delta S^{\ddagger} = -19 \pm 2$ eu. These ac-

(10) Cole-Hamilton, D. J.; Young, R. J.; Wilkinson, G. *J. Chem. Soc., Dalton Trans.* **1976**, 1995.

(11) (a) Hamilton, D. G.; Crabtree, R. H. *J. Am. Chem. Soc.*, in press. We use C = 0.9. (b) Crabtree, R. H.; Lavin, M.; Hamilton, D. G.; Bonneviot, L. *J. Am. Chem. Soc.* **1986**, *108*, 4032.

(12) Kubas, G. J.; Ryan, R. R.; Swanson, B. I.; Vergamini, P. J.; Wasserman, H. J. *J. Am. Chem. Soc.* **1984**, *106*, 451.

(13) Gutowsky, H. S.; Holm, C. H. *J. Chem. Phys.* **1954**, *25*, 122.

tivation parameters may be compared with $\Delta H^{\ddagger} = 15.7 \pm 0.4$ kcal/mol and $\Delta S^{\ddagger} = -4 \pm 1$ eu obtained for the seven-coordinate trifluoroacetate compound $[(CH_3O)_3P]_4MoH(O_2CCF_3)$.[14] The proton line width, $\nu_{1/2}$, is given by $1/\pi T_2$ where T_2 is the spin–spin relaxation time. Because $T_2 \leq T_1$, the minimum possible value of $\nu_{1/2}$ is 5.6 Hz. Thus, the $Os(H_2)$ resonance is broadened due to the short T_1, and it was therefore not possible to follow the dynamic process by ^1H NMR spectroscopy.

The NMR data are insufficient to define a detailed mechanism for the process that permutes the two types of ^{31}P environments. Referring to the solid state structure of **5** determined by X-ray diffraction (vide infra), we note that rotation of the η^2-H_2 ligand, suggested to occur in $[(Ph_2PC_2H_4PPh_2)_2M(H)(\eta^2\text{-}H_2)]BF_4$ (M = Fe, Ru)[15] does not lead to phosphine equivalence. One possible fluxional process, predicated on the assumption that the η^2-H_2 ligand formally occupies two coordination sites, involves the stereochemical nonrigidity associated with seven-coordinate transition metal centers,[14] but this is disfavored by the nearly octahedral metal coordination geometry in **5** and also in $(i\text{-}Pr_3P)_2W(\eta^2\text{-}H_2)(CO)_3$[12] and $[(Ph_2PC_2H_4PPh_2)_2Fe(\eta^2\text{-}H_2)]BF_4$.[15] A more reasonable alternative, consistent with proposed mechanisms for intramolecular hydride scrambling in $M(\eta^1\text{-}H)(\eta^2\text{-}H_2)$ complexes,[11] posits an equilibrium between rigid $(Ph_3P)_3Os(\eta^2\text{-}H_2)(\eta^2\text{-}OAc)^+$ and fluxional, seven-coordinate $(Ph_3P)_3Os(\eta^1\text{-}H)_2(\eta^2\text{-}OAc)^+$. A similar reaction has been proposed to account for intramolecular hydride exchange in $[(c\text{-}C_6H_{11})_2PC_3H_6P(c\text{-}C_6H_{11})_2]PtH_2$,[16] and stereochemically nonrigid, seven-coordinate $(i\text{-}Pr_3P)_2W(CO)_3H_2$ may be observed by NMR to be in equilibrium with $(i\text{-}Pr_3P)_2W(CO)_3(\eta^2\text{-}H_2)$.[17,18]

Derivatization of **5** is achieved by its reaction with acetonitrile, which occurs without evolution of hydrogen, to give *[mer,cis]*-$(Ph_3P)_3OsH(CH_3CN)_2][HC(SO_2CF_3)_2]$ (**6**), eq 2. Formation

$$(Ph_3P)_3Os(H_2)(OAc)^+ + 2CH_3CN \rightarrow (Ph_3P)_3Os(H)(CH_3CN)_2^+ + HOAc \quad (2)$$

of **6** can be viewed as a formal Lewis base induced loss of acetic

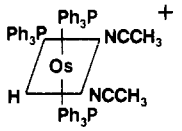

6

acid, a process which confirms that its precursor **5** contained two hydrogen atoms bonded to osmium. The proposed structure of **6** is based on the ^{31}P NMR spectrum in CD_2Cl_2, which displays resonances at 13.9 (d, 2 P, J_{PP} = 18 Hz, J_{PH} = 21 Hz) and 7.6 (t, 1 P, J_{PP} = 18 Hz, J_{PH} = 14 Hz) ppm. In addition, the ^1H NMR spectrum contains a doublet of triplets at −14.8 ppm with J_{PH} = 21 and 14 Hz. These data thus indicate that the hydride is cis to two types of Ph_3P ligands, which are in a 2:1 ratio. The ^1H NMR spectrum also shows singlets at 1.20 and 1.96 ppm in a 1:1 ratio due to the two nonequivalent acetonitrile CH_3CN methyl groups. Unlike $[(Ph_3P)_2RuH(CO)(CH_3CN)_2][HC(SO_2CF_3)_2]$, in which the rate of exchange of coordinated acetonitrile trans to hydride with CD_3CN is faster than that of the cis nitrile,[4] both CH_3CN ligands in **6** equilibrate with CD_3CN within NMR sample preparation time.

Structure of $[(Ph_3P)_3OsH_2(OAc)][HC(SO_2CF_3)_2]$. The osmium coordination core in **5** is shown in Figure 3 with important bond distances and angles being given in Table I. It may be viewed as approximately octahedral with a "vacant" site opposite O1. Attempts to locate the H_2 ligand by using data obtained at −63 °C were unsuccessful as these hydrogens did not refine to a reasonable model. However, molecular hydrogen, like C_2H_2 and C_2H_4, occupies one coordination site in crystallographically characterized dihydrogen complexes,[12,15] and we believe that the H_2 ligand, whose presence is clearly demonstrated by spectroscopic data, occupies the seemingly vacant site trans to O1. In the context of an octahedral metal coordination core that is deformed because of the small bite angle of the η^2-acetate group and the small size of the H_2 ligand, the bond angles make sense. The P1–Os–P2, P1–Os–P3 and P2–Os–P3 angles are 100.89 (3), 98.55 (3) and 158.14 (3)°, respectively; P2 and P3 are bent slightly away from P1. The O1–Os–O2 angle, 59.42 (8)°, is smaller than the idealized value of 90°, doubtless because of the small bite of the planar (maximum displacement from the C1,C2,O1,O2 least-squares plane is 0.004 Å at C1) bidentate acetate ligand. Osmium is displaced by only 0.13 Å from the Os,P1,P2,P3 least-squares plane, and the dihedral angle between this and the acetate least-squares plane is 96°. The Os–P1 bond, 2.325 (1) Å, is significantly shorter than Os–P2 or Os–P3, 2.376 (1) and 2.399 (1) Å, respectively. This may be attributed to the weaker structural trans effect of the acetate oxygen atom O2 (the P1–Os–O2 angle is 151.1 (7)°) compared to that for mutually trans phosphines. Indeed, the Os–O2 bond, 2.198 (2) Å, is much longer than that between the metal and O1, 2.160 (2) Å. The η^2-H_2 ligand is expected to exert a weaker trans effect than a phosphine.

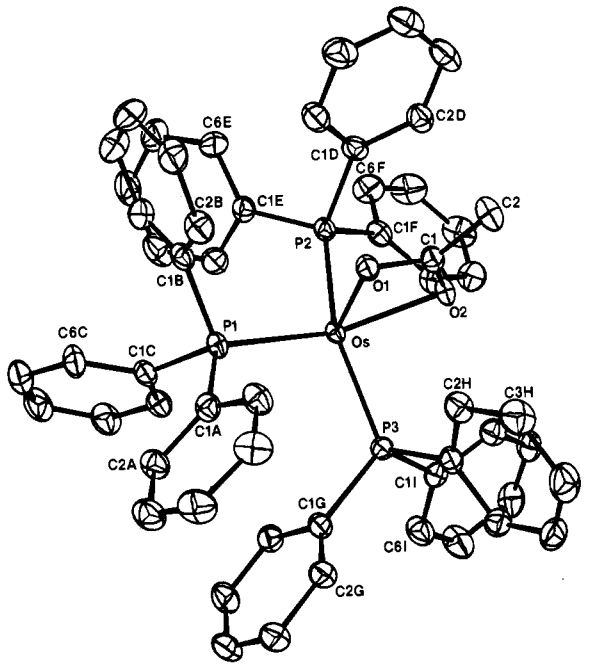

Figure 3. ORTEP view of the $[(Ph_3P)_3Os(\eta^2\text{-}H)_2(\eta^2\text{-}OAc)]^+$ ion in **5**. Ellipsoids are drawn with 50% probability boundaries.

Table I. Selected Bond Distances (Å) and Angles (deg) in $[(Ph_3P)_3Os(H_2)(OAc)][HC(SO_2CF_3)_2]$ and Their Standard Deviations

	Bond Distances		
Os–P1	2.325 (1)	Os–O2	2.198 (2)
Os–P2	2.376 (1)	O1–C1	1.274 (4)
Os–P3	2.399 (1)	O2–C1	1.269 (4)
Os–O1	2.160 (2)	C1–C2	1.481 (5)
	Bond Angles		
P1–Os–P2	100.89 (3)	P3–Os–O2	87.01 (6)
P1–Os–P3	98.55 (3)	O1–Os–O2	59.42 (8)
P1–Os–O1	91.68 (3)	Os–O1–C1	93.0 (2)
P1–Os–O2	151.10 (6)	Os–O2–C1	91.3 (2)
P2–Os–P3	158.14 (7)	O1–C1–O2	116.3 (3)
P2–Os–O1	90.41 (6)	O1–C1–O2	121.7 (3)
P2–Os–O2	80.79 (6)	O2–C1–C2	122.1 (3)
P3–Os–O1	98.94 (6)		

(14) Wreford, S. S.; Kouba, J. K.; Kirner, J. F.; Muetterties, E. L.; Tavanaiepour, I.; Day, V. W. *J. Am. Chem. Soc.* **1980**, *102*, 1588.
(15) Morris, R. H.; Sawyer, J. F.; Shiralian, M.; Zubkowski, J. D. *J. Am. Chem. Soc.* **1985**, *107*, 5581.
(16) Clark, H. C.; Hamden-Smith, M. J. *J. Am. Chem. Soc.* **1986**, *108*, 3829.
(17) Kubas, G. J.; Ryan, R. R.; Wroblewski, D. A. *J. Am. Chem. Soc.* **1986**, *108*, 1339.
(18) Additional reports of interconversion of η^2 and η^1 hydride ligands include (a) Chinn, M. S.; Heinekey, D. M. *J. Am. Chem. Soc.* **1987**, *109*, 5865. (b) Bautista, M.; Earl, K. A.; Morris, R. H.; Sella, A. *J. Am. Chem. Soc.* **1987**, *109*, 3780. (c) Bianchini, C.; Mealli, C.; Peruzzini, M.; Zanobini, F. *J. Am. Chem. Soc.* **1987**, *109*, 5548.

Table II. Core-Level Binding Energies (eV) for Osmium Compounds

compd	Os($4f_{7/2}$)	Os($4f_{5/2}$)	other
Os metal	51.6	54.3	
OsO_2	54.0	56.5	O(1s) 532.0, 533.5
$OsCl_3$	53.6	56.2	Cl($2p_{3/2}$) 198.8
$KOsO_3N$	56.3	60.1	K($2p_{3/2}$) 292.9 O(1s) 532.4 N(1s) 398.8
Os_2NCl_5	57.3[a]	60.0	Cl($2p_{3/2}$) 199.3 N(1s) 399.3
$(Ph_3P)_3OsHBr(CO)$	51.3	54.0	O(1s) 532.7 P(2s) 189.0
$[(Ph_3P)_4OsH_3][HC(SO_2CF_3)_2]$	51.4	54.0	O(1s) 532.3
$[(Ph_3P)_3Os(OAc)(H_2)][HC(SO_2CF_3)_2]$	51.8	54.4	O(1s) 532.3
$(Ph_3P)_3OsH_4$	50.7	53.4	

[a] This compound shows a minor Os species with binding energies of 56.3 and 58.7 eV.

X-ray Photoelectron Spectroscopic Studies. XPS spectra of some osmium complexes were obtained in order to find out if this technique could be used to probe the effective metal oxidation state(s) in **5** and related compounds.[19] The data are summarized in Table II. The Os 4f core binding energies are indeed dependent on *formal* oxidation state provided that the metal is bonded to "hard" ligands such as Cl, O, or N. Thus, the $4f_{7/2}$ energies of Os metal, $OsCl_3$, and $KOsO_3N$ are 51.6, 53.6, and 56.3 eV, respectively. The situation is different when "soft" ligands, i.e. those with greater back-bonding ability, are involved. Ligands such as Ph_3P and CO tend to buffer electron density around osmium so that, regardless of formal oxidation state, the metal core binding energies are approximately constant. Thus, the $4f_{7/2}$ energies for the Os(II) and Os(IV) compounds $(Ph_3P)_3OsHBr(CO)$ and $(Ph_3P)_3OsH_4$ are 51.2 and 50.7 eV, respectively. Phenomenologically, this buffering effect of Ph_3P and CO tends to even out, by XPS criteria, electron density at the metal, and it may be a general feature in organometallic compounds.

Experimental Section

Reactions were carried out, unless otherwise noted, under a water- and oxygen-free nitrogen atmosphere. Toluene was distilled from Na–K alloy. Infrared spectra were recorded on Nujol mulls unless otherwise noted. Bis((trifluoromethyl)sulfonyl)methane was prepared by the method of Koshar and Mitsch;[20] transition metal acetates were synthesized by literature methods.[21]

$[(Ph_3P)_2Ru(CO)_2(OAc)][HC(SO_2CF_3)_2]\cdot C_7H_8$ (1). A mixture of 0.16 g of $(Ph_3P)_2Ru(CO)_2(OAc)_2$ (0.2 mmol), 0.056 g of $H_2C(SO_2CF_3)_2$ (0.2 mmol), and 6 mL of toluene was stirred at 80 °C for 12 h. The product was collected on a filter and washed with more toluene. The yield of white granular solids was 0.2 g (90%). Anal. Calcd for $C_{50}H_{42}F_6O_8P_2RuS_2$: C, 54.0; H, 3.8; Ru, 9.1; P, 5.6; S, 5.8. Found: C, 54.2; H, 4.0; Ru, 9.5; P, 5.6; S, 5.4. ^1H NMR ($CDCl_3$): 3.84 (s, 1, $HC(SO_2CF_3)_2^-$), 2.33 (s, 3, toluene CH_3), 0.45 (s, 3, O_2CCH_3) ppm.

$[(Ph_3P)_4Ru_2(CO)_2(\mu\text{-}H)_2(\mu\text{-}OAc)][HC(SO_2CF_3)_2]$ (3). A mixture of 0.16 g (0.22 mmol) of $(Ph_3P)_2RuH(CO)(OAc)$, 0.063 g (0.22 mmol) of $H_2C(SO_2CF_3)_2$, and 6 mL of toluene was stirred for 0.5 h and then heated at 85 °C with stirring for 12 h. Filtration gave 0.09 g (50%) of **3** as yellow-brown microcrystals. Anal. Calcd for $C_{79}H_{66}O_8P_4Ru_2S_2$: C, 57.6; H, 4.0; Ru, 12.3; P, 7.5; S, 3.9. Found: C, 58.0; H, 4.0; Ru, 12.0; P, 7.1; S, 4.1. Electronic spectrum [CH_2Cl_2, λ_{max} (log ϵ)]: 345 (4.06) and 460 (3.12) nm. ^1H NMR ($CDCl_3$): 3.77, 1.78 ppm. ^{19}F NMR ($CDCl_3$): −80.9 ppm (s).

$[(Ph_3P)_4Ru_2(\mu\text{-}Cl)_2(\mu\text{-}OAc)][HC(SO_2CF_3)_2]$ (4). A mixture of 0.16 g (0.2 mmol) of $(Ph_3P)_2Ru(CO)Cl(OAc)$, 0.56 g (0.2 mmol) of $H_2C(SO_2CF_3)_2$, and 6 mL of toluene was heated at 80 °C for 12 h. Filtration afforded 0.13 g (76%) of **4** as bright yellow microcrystals. Anal. Calcd for $C_{79}H_{64}Cl_2F_6O_8P_4Ru_2S_2$: C, 55.3; H, 3.7; Cl, 4.1; Ru, 11.8; P, 7.2; S, 3.7. Found: C, 54.0; H, 3.7; Cl, 4.0; Ru, 12.3; P, 7.1; S, 3.5. IR: ν_{CO} 1973 cm^{-1}. ^1H NMR ($CDCl_3$): 3.85, 1.99 ppm. ^{31}P NMR ($CDCl_3$): 39.8 (s) ppm.

$[(Ph_3P)_3Os(\eta^2\text{-}H_2)(\eta^2\text{-}OAc)][HC(SO_2CF_3)_2]\cdot C_7H_8$ (5). A mixture of 0.26 g (0.25 mmol) of $(Ph_3P)_3OsH(OAc)$, 0.07 g (0.25 mmol) of $H_2C(SO_2CF_3)_2$, and 3 mL of toluene was stirred at room temperature. The solid phase was collected on a filter, washed with fresh solvent, and vacuum dried to give 0.24 g (73%) of **5** as yellow microcrystals. Solutions of the compound are air sensitive. Anal. Calcd for $C_{66}H_{59}F_6OsO_6P_3S_2$: C, 56.3; H, 4.2, Os, 13.5; P, 6.6; S, 4.5. Found: C, 56.2; H, 4.1; Os, 14.0; P, 7.0; S, 4.5. IR: 2060 (w) (OsH) cm^{-1}. ^1H NMR (CD_2Cl_2): 3.84, 2.33, 1.02 ppm. Crystals used for the X-ray diffraction experiment were grown in a drybox by diffusion of pentane vapor into a dichloromethane solution of the compound.

$[(Ph_3P)_3OsH(CH_3CN)_2][HC(SO_2CF_3)_2]$ (6). A solution of 0.24 g of **5** in 3 mL of acetonitrile (distilled from P_2O_5 under N_2) was stirred for 1 h. Concentration and cooling afforded 0.18 g (75%) of **6** as white, fibrous needles. Anal. Calcd for $C_{61}H_{53}F_6N_2OsO_4P_3S_2$: C, 54.7; H, 4.0; N, 2.1; Os, 14.2; P, 7.0. Found: C, 54.4; H, 4.1; N, 1.9; Os, 14.0; P, 7.2. IR: 2056 (OsH), 2268 (C≡N) cm^{-1}.

NMR Spectra. NMR spectra were obtained on a Varian XL-200 instrument at 200 (^1H) and 80.98 (^{31}P) MHz with CD_2Cl_2 or $CDCl_3$ as solvent. Positive chemical shifts are downfield of internal $(CH_3)_4Si$ and $CFCl_3$ or external 85% H_3PO_4. In all cases, ^{31}P NMR spectra were obtained with both white noise ^1H coupling and with narrow-band decoupling of the aromatic protons.

^{31}P DNMR spectra were obtained on solutions in CD_2Cl_2 with gated ^1H decoupling using a 25% duty cycle to minimize rf heating of the sample and with a 0.4-s acquisition time, 1.1-s delay and 15-μs (60°) pulse. Temperatures were calibrated by substitution of neat methanol for the analytical sample; the spin-decoupler coil was used to observe its ^1H resonance, and temperatures were then determined from the data of Van Geet.[22] Absorptions for the two different types of phosphines were observable between −49 and +12 °C. The chemical shifts showed a temperature dependence of 1.3 Hz/deg. Shifts at higher temperature were determined by linear extrapolation. Lifetimes were calculated by using the equations of Gutowsky and Holm[13] to simulate the spectra. The calculations were performed using an Apple II(+) microcomputer program, which adjusted both the lifetime and chemical shifts (below coalescence) for the best fit to the line width and apparent peak separation in the observed spectrum.[23] Errors were calculated as before[24] but assuming a maximum systematic error in temperature of ±2 °C. These errors are small because the chemical shift difference between the two exchanging sites is >200 Hz at low temperature. The small P–P coupling was neglected, but the line width in the absence of exchange was increased from 2 Hz at 40 °C to 10 Hz at 10 °C to correct for this.

Spin–lattice relaxation times were measured at 400 MHz over 20 °C intervals. The spectrometer thermocouple was calibrated by using a sample of neat methanol. The standard 180°–τ–90° pulse sequence was employed with a recycle delay at least 6 times T_1. A composite pulse was used for the 180° pulse to compensate for off-resonance effects. Ten measurements were obtained for τ between 5 ms and 0.4 s for **5** and between 20 ms and 1.0 s for $[(Ph_3P)_4OsH_3][HC(SO_2CF_3)_2]$. Relaxation times were calculated by using a three-parameter fit to the peak intensities.

X-ray photoelectron spectra were obtained on a Hewlett-Packard 5950B instrument operating at 1×10^{-9} mm base pressure during data collection and employing a monochromatized Al $K\alpha_{1,2}$ radiation source operated at 800 W emissive power. Resolution for a 83.95 eV Au($4f_{7/2}$) reference line was ±0.10 eV with a fwhm of 0.80 eV. Samples were mounted on Scotch Brand 665 double-coated tape. Surface charging was

(19) Core binding energies for a very great variety of transition-metal complexes have been published: Feltham, R. D.; Brant, P. *J. Am. Chem. Soc.* **1982**, *104*, 641.
(20) Koshar, R. J.; Mitsch, R. A. *J. Org. Chem.* **1973**, *38*, 3358.
(21) Robinson, S. D.; Utley, M. F. *J. Chem. Soc., Dalton Trans.* **1973**, 1912.
(22) van Geet, A. L. *Anal. Chem.* **1971**, *43*, 679.
(23) Newmark, R. A. *J. Chem. Educ.* **1983**, *60*, 45.
(24) Siedle, A. R.; Newmark, R. A.; Kruger, A. A.; Pignolet, L. H. *Inorg. Chem.* **1981**, *20*, 3399.

Table III. Summary of Crystal Data and Intensity Collection for $[(Ph_3P)_3Os(\eta^2\text{-}H_2)(OAc)][HC(SO_2CF_3)_2]\cdot C_7H_8$ (**5**)

Crystal Parameters	
cryst syst	triclinic
space group	$P\bar{1}$ (No. 2)
cell params (−63 °C; +25 °C)	
a, Å	14.780 (4); 14.912 (2)
b, Å	15.376 (5); 15.46 (1)
c, Å	13.854 (4); 13.987 (4)
α, deg	100.62 (2); 100.74 (5)
β, deg	97.63 (2); 97.42 (2)
γ, deg	77.36 (2); 77.34 (5)
V, Å^3	3005 (3); 3079 (4)
Z	2
calcd density, g cm^{-3}	1.557
abs coeff, cm^{-1}	23.37
cryst dimens, mm	0.35 × 0.20 × 0.05
max, min, av transmissn factors	1.0, 0.76, 0.88
formula	$OsS_2P_3F_6O_6C_{66}H_{59}$
fw	1409.4
Measurement of Intensity Data (−63 °C)	
diffractometer	CAD 4
radiation	Mo K$\bar{\alpha}$ (λ = 0.71069 Å)
scan type (2θ range, deg)	ω–2θ (0–56)
no. of unique reflcns measd (region)	14955 (h,±k,±l)
obsd[a]	12055 [$F_o^2 \geq \sigma(F_o^2)$]
refinement by full-matrix least squares	
no. of params	757
R[b]	0.036
R_w[b]	0.041
GOF[b]	1.30
p[a]	0.04

[a] The intensity data were processed as described in: *CAD 4 and SDP-PLUS User's Manual*; B. A. Frenz & Assoc.: College Station, TX, 1982. The net intensity $I = [K(\text{NPI})](C - 2B)$, where K = 20.1166 × attenuator factor, NPI = ratio of fastest possible scan rate to scan rate for the measurement, C = total count, and B = total background count. The standard deviation in the net intensity is given by $[\sigma(I)]^2 = (K/\text{NPI})^2[C + 4B + (pI)^2]$, where p is a factor used to downweight intense reflections. The observed structure factor amplitude F_o is given by $F_o = (I/Lp)$, where Lp = Lorentz and polarization factors. The $\sigma(I)$'s were converted to the estimated errors in the relative structure factors $\sigma(F_o)$ by $\sigma(F_o) = [\sigma(I)/I]F_o$. [b] The function minimized was $\sum w(|F_o| - |F_c|)^2$, where $w = 1/[\sigma(F_o)]^2$. The unweighted and weighted residuals are defined as $R = \sum(||F_o| - |F_c||)/\sum|F_o|$ and $R_w = [(\sum w(|F_o| - |F_c|))^2/(\sum w|F_o|^2)^2]^{1/2}$. The error in an observation of unit weight (GOF) is $[\sum w(|F_o| - |F_c|)^2/(\text{NO} - \text{NV})]^{1/2}$, where NO and NV are the numbers of observations and variables, respectively.

controlled by use of a low-energy electron flood gun operated at 0.4 mA current and 2 eV voltage. Charge-corrected binding energies are expressed relative to the background C(1s) line at 285.0 eV.

Collection and Reduction of X-ray Data. A summary of crystal and intensity data is given in Table III. A crystal of **5** was secured to the end of a glass fiber by and coated with epoxy resin and maintained at −63 ± 1 °C during line up and data collection. The crystal was found to belong to the triclinic class by the Enraf-Nonius CAD 4–SDP peak search, centering, and indexing programs.[25] Background counts were measured at both ends of the scan range and are equal, at each side, to one-fourth of the scan range of the peak. In this manner, the total duration of background measurements is equal to half of the time required for the peak scan. The intensities of three standard reflections were measured every 1.5 h of X-ray exposure, and no decay was noted. The data were corrected for Lorentz, polarization, and background effects. An empirical absorption correction was applied by using the SDP programs PSI and EAC.[25]

Solution and Refinement of the Structure. The structure was solved by conventional heavy-atom techniques. The Os atom was located by a Patterson synthesis. Full-matrix least-squares refinement and difference-Fourier calculations were used to locate all the remaining non-hydrogen atoms. The atomic scattering factors were taken from the usual tabulation,[26] and the effects of anomalous dispersion were included in F_c by use of Cromer and Ibers'[27] values of $\Delta f'$ and $\Delta f''$. In the final

Table IV. Positional Parameters and Their Estimated Standard Deviations for the Cation of **5**[a]

atom	x	y	z	B, Å^2
Os	0.30543 (1)	0.22020 (1)	0.16929 (1)	1.166 (2)
P1	0.19008 (6)	0.34993 (6)	0.16717 (7)	1.44 (2)
P2	0.21572 (6)	0.10641 (6)	0.11589 (7)	1.46 (2)
P3	0.43139 (6)	0.28901 (6)	0.25249 (7)	1.39 (2)
O1	0.3301 (2)	0.2186 (2)	0.0187 (2)	1.57 (5)
O2	0.4114 (2)	0.1137 (2)	0.0969 (2)	1.75 (5)
C1	0.3923 (3)	0.1465 (2)	0.0173 (3)	1.61 (7)
C2	0.4402 (3)	0.1042 (3)	−0.0722 (3)	2.32 (8)
C1A	0.2369 (3)	0.4511 (2)	0.1654 (3)	1.85 (7)
C2A	0.2104 (3)	0.5317 (3)	0.2286 (3)	2.12 (8)
C3A	0.2490 (3)	0.6058 (3)	0.2247 (3)	2.64 (9)
C4A	0.3119 (3)	0.5998 (3)	0.1581 (3)	2.89 (9)
C5A	0.3397 (3)	0.5195 (3)	0.0964 (3)	2.61 (8)
C6A	0.3026 (3)	0.4453 (3)	0.1000 (3)	2.19 (8)
C1B	0.1132 (3)	0.3409 (2)	0.0517 (3)	1.78 (7)
C2B	0.1398 (3)	0.3559 (3)	−0.0365 (3)	2.38 (8)
C3B	0.0812 (3)	0.3459 (3)	−0.1234 (3)	2.79 (9)
C4B	−0.0032 (3)	0.3215 (3)	−0.1243 (3)	3.2 (1)
C5B	−0.0304 (3)	0.3064 (3)	−0.0388 (4)	3.1 (1)
C6B	0.0282 (3)	0.3147 (3)	0.0487 (3)	2.28 (8)
C1C	0.1051 (3)	0.3883 (2)	0.2585 (3)	1.84 (7)
C2C	0.1171 (3)	0.3559 (3)	0.3475 (3)	2.00 (7)
C3C	0.0483 (3)	0.3832 (3)	0.4120 (3)	2.74 (9)
C4C	−0.0331 (3)	0.4428 (3)	0.3882 (3)	2.98 (9)
C5C	−0.0446 (3)	0.4778 (3)	0.3011 (3)	2.83 (9)
C6C	0.0247 (3)	0.4514(3)	0.2372 (3)	2.35 (8)
C1D	0.2180 (3)	0.0607 (2)	−0.0153 (3)	1.70 (7)
C2D	0.2722 (3)	−0.0240 (3)	−0.0475 (3)	2.16 (8)
C3D	0.2773 (3)	−0.0543 (3)	−0.1485 (3)	2.77 (9)
C4D	0.2305 (3)	−0.0019 (3)	−0.2159 (3)	3.03 (9)
C5D	0.1778 (3)	0.0824 (3)	−0.1842 (3)	3.0 (1)
C6D	0.1727 (3)	0.1138 (3)	−0.0848 (3)	2.33 (8)
C1E	0.0951 (3)	0.1271 (2)	0.1417 (3)	1.75 (7)
C2E	0.0775 (3)	0.1585 (3)	0.2394 (3)	2.34 (8)
C3E	−0.0112 (3)	0.1732 (3)	0.2678 (4)	3.07 (9)
C4E	−0.0840 (3)	0.1563 (3)	0.1984 (4)	3.4 (1)
C5E	−0.0679 (3)	0.1239 (3)	0.1005 (4)	3.3 (1)
C6E	0.0218 (3)	0.1089 (3)	0.0717 (3)	2.56 (9)
C1F	0.2621 (3)	0.0060 (2)	0.1737 (3)	1.89 (7)
C2F	0.3516 (3)	−0.0112 (3)	0.2202 (3)	2.30 (8)
C3F	0.3857 (3)	−0.0907 (3)	0.2588 (3)	2.67 (9)
C4F	0.3307 (4)	−0.1538 (3)	0.2511 (3)	3.1 (1)
C5F	0.2417 (4)	−0.1377 (3)	0.2057 (4)	3.4 (1)
C6F	0.2072 (3)	−0.0583 (3)	0.1668 (3)	2.69 (9)
C1G	0.4069 (3)	0.3979 (2)	0.3324 (3)	1.65 (7)
C2G	0.4493 (3)	0.4689 (3)	0.3263 (3)	1.98 (7)
C3G	0.4315 (3)	0.5500 (3)	0.3913 (3)	2.49 (9)
C4G	0.3714 (3)	0.5599 (3)	0.4625 (3)	2.78 (9)
C5G	0.3278 (3)	0.4909 (3)	0.4693 (3)	2.54 (9)
C6G	0.3448 (3)	0.4100 (3)	0.4046 (3)	1.95 (7)
C1H	0.5293 (3)	0.2967 (2)	0.1879 (3)	1.69 (7)
C2H	0.5209 (3)	0.2948 (3)	0.0858 (3)	2.11 (8)
C3H	0.5979 (3)	0.2980 (3)	0.0395 (3)	2.87 (9)
C4H	0.6816 (3)	0.3064 (3)	0.0941 (4)	3.01 (9)
C5H	0.6893 (3)	0.3092 (3)	0.1943 (3)	2.51 (9)
C6H	0.6146 (3)	0.3037 (3)	0.2422 (3)	2.06 (8)
C1I	0.4927 (3)	0.2122 (2)	0.3379 (3)	1.63 (7)
C2I	0.5323 (3)	0.1241 (3)	0.2973 (3)	2.16 (8)
C3I	0.5736 (3)	0.0606 (3)	0.3571 (3)	2.44 (8)
C4I	0.5775 (3)	0.0841 (3)	0.4579 (3)	2.69 (9)
C5I	0.5400 (4)	0.1718 (3)	0.4996 (3)	3.0 (1)
C6I	0.4986 (3)	0.2357 (3)	0.4397 (3)	2.40 (8)

[a] All atoms are refined with anisotropic thermal parameters and B values are given in the form of the isotropic equivalent thermal parameter defined as $^4/_3[a^2B(11) + b^2B(22) + c^2B(33) + ab(\cos\gamma)B(12) + ac(\cos\beta)B(13) + bc(\cos\alpha)B(23)]$. Parameters of all atoms are given in the supplementary material.

(25) All calculations were carried out on PDP 8A and 11/34 computers with use of the Enraf-Nonius CAD 4-SDP programs. This crystallographic computing package is described by: Frenz, B. A. In *Computing in Crystallography*; Shenk, H., Olthof-Hazekamp, R., van Konigsveld, H., Bassi, G. C., Eds.; Delft University Press: Delft, Holland, 1978; pp 64–71. See also: *CAD 4 and SDP User's Manual*; Enraf-Nonius: Delft, Holland, 1978.

(26) Cromer, D. T.; Waber, J. T. *International Tables for X-Ray Crystallography*; Kynoch: Birmingham, England, 1974; Vol. IV, Table 2.2.4.

least-squares cycle, the largest parameter shift was 0.02 times its estimated esd. Phenyl hydrogen atom positions were calculated (d_{C-H} set at 0.95 Å) and included in structure factor calculations but were not refined. The final difference Fourier map revealed an electron density peak in the region where the η^2-H_2 ligand was expected. The maximum in this area was positioned 1.6 Å from the Os atom approximately trans to O1 (O1-Os-peak = 170°). Other relevant angles about Os to this peak were 86° to P1, 80° to P2, 88° to P3 and 129° to O2. Attempts to refine this peak as a hydrogen atom or as a η^2-H_2 ligand were unsuccessful and upon careful examination of the electron density in this region, contours expected for a H_2 ligand were not observed. It was concluded that the presence of the heavy atoms in the structure precluded its resolution. The largest peaks in the final difference Fourier map were located approximately 0.9 Å from the Os atom and were about 2 electron Å^{-3}, compared with 0.9 electron Å^{-3} for the suspected η^2-H_2.

The final positional and thermal parameters of the refined atoms appear in Table IV. A table of observed and calculated structure factor amplitudes is available as supplementary material.

Acknowledgment. We are grateful to members of the 3M Analytical and Properties Research Laboratory for spectroscopic and analytical data, to Robert Koshar, 3M Industrial and Consumer Sector Research Laboratory, for gifts of fluorocarbon acids, and to Prof. R. H. Crabtree for communicating some of his results prior to their publication. L.H.P. acknowledges support from the National Science Foundation and the donors of the Petroleum Research Fund, administered by the American Chemical Society, for his contribution to this work.

(27) Cromer, D. T.; Ibers, J. A. In ref 26.

Registry No. **1**, 113220-61-4; **3**, 113220-59-0; **4**, 113250-53-6; **5**, 113250-56-9; **6**, 113220-65-8; $(Ph_3P)_2Ru(CO)_2(OAc)_2$, 31267-49-9; $H_2C(SO_2CF_3)_2$, 428-76-2; $(Ph_3P)_2RuH(CO)(OAc)$, 50661-73-9; $(Ph_3P)_2Ru(CO)Cl(OAc)$, 34808-05-4; $(Ph_3P)_3OsH(OAc)$, 50894-84-3; $[(Ph_3P)_3Os(\eta^2\text{-}HD)(\eta^2\text{-}OAc)][PhC(SO_2CF_3)_2]$, 113220-63-6; $PhCD(SO_2CF_3)_2$, 113250-57-0.

Supplementary Material Available: Tables of positional and thermal parameters (complete listing), general temperature factor expressions, and distances and angles within the phenyl rings, $HC(SO_2CF_3)_2^-$ anion, and toluene solvate molecule (13 pages); a table of observed and calculated structure factor amplitudes (49 pages). Ordering information is given on any current masthead page.

Contribution from the Departamento de Química Inorgánica, Facultad de Química, Universidad de Sevilla, Instituto de Ciencias de Materiales de Sevilla, CSIC, Apto. 553, Sevilla, Spain, and Department of Chemistry, Northern Illinois University, DeKalb, Illinois 60115

Synthesis, Characterization, and Properties of the η^2-Acyl Complexes $Mo(\eta^2\text{-}COCH_2CMe_3)X(PMe_3)_4$ (X = Cl, Br)

Ernesto Carmona,*[1a] Miguel A. Muñoz,[1a] and Robin D. Rogers*[1b]

Received June 16, 1987

The η^2-acyl complexes of molybdenum $Mo(\eta^2\text{-}COCH_2CMe_3)X(PMe_3)_4$ (X = Cl (**1a**), Br (**1b**)) have been prepared by the action of $Mg(CH_2CMe_3)X$ on the carbonyl carbonate $Mo(CO_3)(CO)(PMe_3)_4$. Complex **1** decomposes in solution with dissociation of PMe_3. This reaction occurs faster in the presence of small amounts of water (2-3 drops) with formation of the hydroxo species $[MoX(CO)(PMe_3)_2(\mu\text{-}OH)]_2$ (X = Cl (**2a**), Br (**2b**)). Carbonylation of **1a**, at room temperature and pressure, affords successively $Mo(\eta^2\text{-}COCH_2CMe_3)Cl(CO)(PMe_3)_3$ and $Mo(\eta^2\text{-}COCH_2CMe_3)Cl(CO)_2(PMe_3)_2$. Finally, the reaction of $Mo(CO_3)(CO)(PMe_3)_4$ with CH_2Cl_2 yields the 7-coordinate anionic compound $MoCl_3(CO)(PMe_3)_3$, which is isolated as the tetramethylphosphonium salt, $[PMe_4][MoCl_3(CO)(PMe_3)_3]$ (**3**). The crystal structure of **1b** has been determined by X-ray crystallography. It crystallizes in the orthorhombic space group, $P2_12_12_1$, with a = 10.021 (2) Å, b = 16.752 (3) Å, c = 16.855 (5) Å, and D_{calcd} = 1.36 g cm^{-3} for Z = 4. A total of 1098 independent observed [$F_o \geq 5\sigma(F_o)$] reflections were used in the least-squares refinement, which led to a final conventional R value of 0.051. The molybdenum atom has an approximate pentagonal-bipyramidal geometry, the η^2-acyl ligand residing in the pentagonal plane. The acyl and bromo ligands are trans; important distances include Mo-Br = 2.687 (5) Å, Mo-C = 2.00 (3) Å, Mo-O = 2.21 (2) Å, and Mo-P = 2.48 (4) Å, average.

Introduction

η^2-Acyl complexes of molybdenum have been relatively uncommon until very recently, the first compound of this type being the chloride-bridged, dinuclear species $[Mo(\eta^2\text{-}COCH_2SiMe_3)(CO)_2(PMe_3)(\mu\text{-}Cl)]_2$.[2] Later work from our laboratory has resulted in the characterization of the formally 6-coordinate mononuclear complexes $Mo(\eta^2\text{-}COR)X(CO)(PMe_3)_3$ and of other related compounds,[3] while the groups of Lalor and Ferguson,[4] Curtis,[5] and Templeton[6] have effected the characterization of the complexes $TpMo(\eta^2\text{-}COR)(CO)_2$ (Tp = hydridotris(pyrazolyl)borate ligand) and of other similar species.

Scheme I

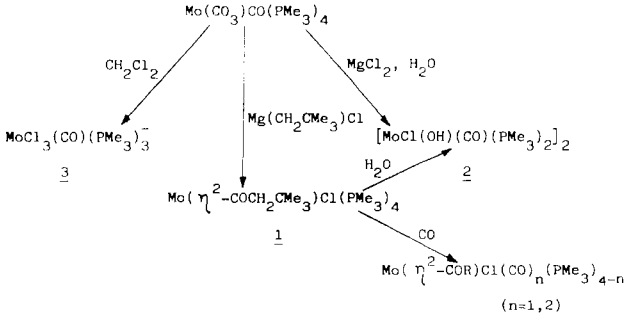

We are currently studying[7] the influence of steric and electronic effects on the relative stability of 7-coordinate alkyl carbonyl complexes, LnM(CO)R, and isomeric 6-coordinate η^2-acyls,

(1) (a) Universidad de Sevilla. (b) Northern Illinois University.
(2) Carmona, E.; Wilkinson, G.; Rogers, R. D.; Hunter, W. D.; Zawarotko, M. J.; Atwood, J. L. *J. Chem. Soc., Dalton Trans.* **1980**, *229*.
(3) Carmona, E.; Sánchez, L.; Marín, J. M.; Poveda, M. L.; Atwood, J. L.; Priester, R. D.; Rogers, R. D. *J. Am. Chem. Soc.* **1984**, *106*, 3214.
(4) Desdmond, T.; Lalor, F. J.; Ferguson, G.; Ruhl, B.; Parvez, M. *J. Chem. Soc., Chem. Commun.* **1983**, 55.
(5) Curtis, M. D.; Shiu, K. B.; Butler, W. B. *J. Am. Chem. Soc.* **1986**, *108*, 1550.
(6) Rusik, C. A.; Tonker, T. L.; Templeton, J. L. *J. Am. Chem. Soc.* **1986**, *108*, 4652.
(7) Carmona, E.; Sánchez, L., to be submitted for publication.

0020-1669/88/1327-1598$01.50/0